Fluorescence-Activated Droplet Sorting of Polyethylene terephthalate Degrading Enzymes

Yuxin Qiao[1,5], Ran Hu[1,4], Dongwei Chen[1, 5], Li Wang[1], Ye Fu[2], Chunli Li[1], Zhiyang Dong[1], Yunxuan Weng[2]*, Wenbin Du[1,3, 4, 5]*

[1] State Key Laboratory of Microbial Resources, Institute of Microbiology, Chinese Academy of Sciences, Beijing 100101, China

[2] Beijing Key Laboratory of Quality Evaluation Technology for Hygiene and Safety of Plastics, Beijing Technology and Business University, Beijing 100048, China

[3] Savid Medical School, University of the Chinese Academy of Sciences, Beijing 100049, China

[4] Department of Life Sciences, University of the Chinese Academy of Sciences, Beijing 100049, China

[5] State Key Laboratory of Transducer Technology, Institute of Microbiology, Chinese Academy of Sciences, Beijing 100101, China

* Corresponding author: wyxuan@th.btbu.edu.cn (Y.X.W.), wenbin@im.ac.cn (W. D.)

Abstract

It is a great challenge to expand the spectrum of enzymes that can decompose synthetic plastics such as Polyethylene terephthalate (PET). However, a bottleneck remains due to the lack of techniques for detecting and sorting environmental microorganisms with vast diversity and abundance. Here, we developed a fluorescence-activated droplet sorting (FADS) pipeline for high-throughput screening of PET-degrading microorganisms or enzymes (PETases). The pipeline comprises three steps: generation of droplets encapsulating single cells, picoinjection of Fluorescein dibenzoate (FDBz) as the fluorogenic probe, and screening of droplets to obtain PET-degrading cells. We characterized critical factors associated with the method, including specificity and sensitivity for discriminating PETase from other enzymes, and optimized its

performance and compatibility with environmental samples. The system was used to screen an environmental sample from a PET textile mill, successfully obtained PET-degrading species belonging to 9 different genera. Moreover, two putative PETases from isolates *Kineococcus endophyticus* Un-5 and *Staphylococcus epidermidis* Un-C2-8 were genetically derived, heterologously expressed, and preliminarily validated for PET-degrading activities. We speculate the FADS pipeline can be widely adopted to discover new PET-degrading microorganisms and enzymes from various environments, as well as directed evolution of PETases using synthetic biology.

KEYWORDS: Droplet microfluidics; Fluorescence-Activated Droplet Sorting; Fluorescein dibenzoate (FDBz); Polyethylene terephthalate (PET); PETases

1. Introduction

Synthetic plastics have become an indispensable part of modern life. The problem of plastic pollution is deepening, especially after the COVID-19 (Coronavirus disease 2019) pandemic broke out[1]. Due to its excellent chemical durability and thermal properties, Polyethylene terephthalate (PET) has become the primary thermoplastic resin for making bottles and fibers[2]. The control, recycling, and treatment of PET wastes have become a great challenge. As a result, significant interests have arisen in unveiling biodegradation of PET by microorganisms to tackle the problems caused by PET wastes[3]. Only a few microbial PET-degrading enzymes (PETases) have been reported, including cutinases-like enzymes from *Thermobifida*[4-5] and lipases or esterases from *Candida antarctica*[6] and *Yarrowia lipolytica*[7]. A PETase derived from *Ideonella sakaiensis* has been found that degrades PET into mono(2-hydroxyethyl) terephthalate (MHET) and terephthalic acid (TPA)[3, 8]. DuraPETase[9], EXO-PETase[10], and leaf-branch compost cutinase (LCC)[11] were recently developed by structure-based protein engineering to improve catalytic activity and thermostability. Despite all these breakthrough, we expect that much more microbial PETases are not yet been discovered according to the great genetic diversity and abundance of

microorganisms in nature. However, discovering new PETases from the environments is time-consuming and labor intensive[12], involving enrichment, screening, cultivation, enzyme expression, and activity validation. Especially, the screening of novel degrading microbes and enzymes remains a slow and complex process due to the inefficiency of current sorting techniques[12]. Traditional measurements for plastic biodegradation include plastic weight loss, changes in the mechanical properties or the chemical structure, and carbon dioxide emission, which take up to several months. High-performance liquid chromatography (HPLC) or absorbance assays have been developed for PET film hydrolysis[15] but have not yet been scaled up for high-throughput analysis of environmental microbial communities or mutant libraries. It is still difficult to quickly evaluate the activity of PETases due to the lack of rapid, specific, sensitive, and quantitative detecting and sorting methods.

To overcome the bottleneck for the screening of functional microbes or enzymes, various high throughput screening techniques have been developed[16-17]. Among them, microfluidic fluorescence-activated droplet sorting (FADS) was introduced to dramatically simplify the operations, improve sorting efficiency and flexibility, and reduce the cost of large library screening[18-19]. FADS has been successfully applied in screening of lipase/esterase[20], DNA/XNA polymerase[21], cellulase[22], and NAD(P)-dependent oxidoreductases[23] by incorporating highly sensitive and specific fluorescent enzymatic assays[24]. In this work, we developed a FADS-based approach for expediting the search of PETases, validated its performance by benchmark PETases, applied it to obtain PET-degrading microbes from the wastewater of a PET textile mill, and evaluated putative new PETases for PET-degrading activities. We envision that the FADS pipeline developed in this study can be widely applied to discovering PET-degrading microorganisms and enzymes.

Results and Discussion

3.1 FADS pipeline for PETases

We established a complete FADS pipeline for sorting of PET-degrading microbes, or PETases

consists of four consecutive steps (**Fig. 1A**): **(1)** The microbial suspension are separated as single cells in picoliter droplets by droplet maker device. PET-degrading species were provided with a suitable long-term incubation without interference by competing species. **(2)** The droplets were re-injected into the picoinjection device to introduce picoliter FDBz into each droplet and incubated at room temperature for a short time to allow the lipolysis of FDBz. **(3)** The droplets were re-injected into the sorting device for high-throughput sorting to obtain microbial species capable of decomposing FDBz (the fluorogenic probe for PETases). **(4)** The positive droplets were demulsified, and the positive species were isolated and identified on BHET agar plates. Afterward, The PET degradation performances of positive isolates were evaluated by fermentation with PET fibers and observation of surface erosion of PET films.

3.2 New fluorogenic assays for PETases in picoliter droplets

To develop a rapid, sensitive, and specific fluorogenic assay for droplet-based single-cell sorting of PETases, the following criteria have to be met: (1) Structure similarity between the fluorogenic probe and PET polymer structure; (2) good sensitivity and specificity for fluorescence discrimination of PETases from other enzymes; (3) Low level of self-hydrolysis, leakage and cross-talk of the fluorogenic probe and its hydrolyzed products between droplets. Most microbial-oriented PETases catalyze the hydrolysis of ester bonds of PET next to the benzene rings (**Fig. 1B**). We select FDBz as the candidate fluorogenic probe and evaluated its specificity and sensitivity for fluorescence detection of PETases in picoliter droplets. Previous reported, FDBz is not a highly reactive substrate of common lipases and can not be used to stain cancer cells or plant pollen cells[25]. However, FDBz has PET-like ester bonds linked with a benzene group and can likely be hydrolyzed by PETases to generate (FMBz) and fluorescein (**Fig. 1C**), which can be fluorescently detected. We used benchmark PETase and lipase to test the specificity of FDBz in selective reaction with PETases. We performed colorimetric assays, fluorometric analysis, and the droplet-based catalytic reaction of benchmark PETases using FDBz as the substrate. The colorimetric assays were performed in Eppendorf tubes by mixing 250 μM FDBz with various enzyme solutions separately, including cutinase (10 μM, a positive PETase),

lipase (10 μM, the negative control), and Tris-HCl buffer (the blank control). After 2-hour incubation, only the tube with cutinase turned yellow and fluorescence, while the tubes with lipase and the control remained unchanged (see **Fig. S3**). Next, quantitative fluorometric analyses were performed using the same reaction setting on a plate reader at an excitation wavelength of 488 nm and an emission wavelength of 523 nm. During 2-h incubation at 37 ^{o}C, the fluorescence intensity of microwells with cutinase (green line) increased nearly 346.5-fold, compared to 19.9-fold increase with lipase (grey line); the blank control (black line) remained flat during 2-h incubation, indicate high specificity and substrate selectivity of cutinase-FDBz hydrolysis (**Fig. 2A**). We further studied the effect of cutinase concentration on FDBz hydrolysis. As shown in Fig. 2B, the fitted dose-response curve is in good agreement with classical Michaelis Menten enzymatic kinetics (R^2=1) (**Fig. 2B**).

To evaluate if FDBz is suitable for droplet-based PETase screening, we performed assays by mixing FDBz with either cutinase or lipase to make positive and negative droplets at a volume of 4 pL separately to yield final concentrations of 125-μM FDBz and 5-μM cutinase or lipase. First, we used the FADS optical system to read 40-min incubated positive or negative droplets separately with the same setting. The intensity histogram showed that signals of positive droplets are in the range of 2.0×10^6 to 8.5×10^6, and the signal of negative droplets are in a much lower range of 1.0×10^4 to 5.0×10^4 (**Fig. S4**). The difference of fluorescence intensities allows absolute threshold setting to discriminate PETases from common lipases and a sorting throughput of 700 droplets per second with sorting efficiency >98.8% using our FADS system[20]. Afterward, positive and negative droplets are mixed, and monolayer arrays of droplets were prepared for time-lapse fluorescence imaging to investigate the leakage and self-hydrolysis (**Fig. 2C**). The ratio of fluorescence intensities of positive droplets against negative droplets decreased from 20.88 to 11.49 after 2-h co-incubation (**Fig. 2D**) but is still sufficient for absolute discrimination of droplets. Overall, similar results were found in bulk and droplet-based assays, proving that FDBz is qualified as a specific fluorogenic substrate of PETases.

3.3 FADS of PET-degrading microbes from an environmental sample

We applied the FADS pipeline to screen PET-degrading microbes from the wastewater of a PET textile mill located in Shaoxing city (Zhejiang, China). Bacterial suspensions of the original samples and its enrichment culture were screened to discover new PET-degrading microbes and PETases (**Fig. 3A, 3B**). The FADS was performed at a throughput of 700 drops per second for several hours. As we expected, after enrichment cultivation, the positive rates with droplet fluorescence above the sorting threshold increased to 2.98%, compared with 0.27% of original samples using the same conditions (**Fig. 3A, B**). The sorted positive droplets were then demulsified and subjected for cultivation on agar plates. In total, we obtained 17 potential PET-degrading isolates belonging to eight genera, including nine isolates from the original sample and six isolates from the PET-YSV enrichment (**Table S1**). Interestingly, the isolated species from the original sample are different from those obtained from the PET-YSV enrichment, which indicates that the enrichment cultivation may lead to the rapid growth of fast-growing opportunistic strains and suppressed the original PET-degrading species which might have slower growth rates.

We use the hydrolysis of BHET on agar plates to preliminarily evaluate the degrading activity of obtained microbial strains. Bacterial BHET-hydrolysis activity was determined by forming clear zones around the punched holes on both BHET agar plates. Among nine strains tested positive for clear-zone formations (**Fig. 3C**, **Table S1**), *Kineococcus endophyticus* Un-5 and *Staphylococcus epidermidis* Un-C2-8 exhibited the highest degrading activity and were selected for further degradation evaluation.

To further confirm the degradation activity, isolates Un-C2-8 and Un-5 were inoculated in 20 mL YSV medium, added with 40 mg PET films, and cultivated at 37 °C. After two weeks, the hydrolyzed products, including BHET, MHET, and TPA, were quantified by HPLC. The HPLC profiles revealed that TPA and MHET in Un-C2-8 and Un-5 cultures were much higher than those of *E. coli* and blank control. The total amounts of released products (including TPA and MHET) reached up to 16.68 μg and 1.55 mg for Un-C2-8 and Un-5, respectively (**Fig.4 A, B**). Meanwhile,

similar degradation activities were also observed for both strains when cultivated with 60 mg PET fibers serve as the carbon source in YSV medium (**Fig. S6**). The yields of TPA were 37.63±1.45 μg and 50.98±3.70 μg for Un-C2-8 and Un-5, and MHET were 14.39±0.96 μg, and 16.20±7.54 μg for Un-C2-8 and Un-5, respectively.

To further confirm the biodegradation of PET by the microbial isolates, the PET films were recovered from the flasks cultivating with Un-C2-8, Un-5, and controls for SEM imaging after two weeks. As shown in **Fig. 4C**, distinctly mottled surface erosions of PET films by strains Un-C2-8 and Un-5 were observed compared with the smooth surface of PET film incubated with *E. coli* or blank YSV medium. Un-C2-8 displayed an immersive erosion pattern, which is more likely to secret enzymes to degrade PET film. In some cases, the attached Un-C2-8 cells caused surface erosion and broke the PET film into several pieces (**Fig. S7**). In contrast, Un-5 showed regional surface erosion, which might form bacterial biofilms attached with the surface and forms erosion hot spots (**Fig. 4C**).

3.4 Characterization of putative PETases

Following sequence interpretation of whole-genome sequences of Un-5 and Un-C2-8 and database searching, two putative PETases were selected: S9_948 belonging to the carboxylesterase family found in the genomes of both strains, and PHB belonging to the dienelactone hydrolase family that was found in the genome of Un-5. The amino acid sequence of PHB is compared with those of a carboxylesterase from *Cereibacter sphaeroides* (PDB:4FHZ)[26], a carboxyl esterase from *Rhodobacter sphaeroides* 2.4.1 (PDB: 4FTW), a metagenome-derived esterase (PDB: 3WYD)[27]. and a metagenome-derived esterase LC-Est5 (**Fig. S8**). PHB has a putative 28-residue signal peptide at their N-termini, suggesting that it is secretory proteins like LC-Est1 (AIT56387.1, 25-residue signal peptide). Three amino acid residues that form a catalytic triad of esterolytic/lipolytic enzymes are fully conserved as Ser163, Asp220 in PHB. (Ser165, Asp216, His248 in 4FHZ; Ser117, Asp165, and His197 in 3WYD). A pentapeptide GxSxG motif containing a catalytic serine residue is also conserved as GFSNG (residues 161–165) in PHB (**Fig.**

S8). However, the heterologous expression of PHB in *BL21(DE3)* is not successful, possibly due to its inhibitory effect on the growth of host cells.

As expected for an α/β-hydrolase, the sequence of S9_948 contains the conserved Gly-X-Ser-X-Gly motif (GQSAG), which includes the catalytic serine residue (**Fig. S9**). The esterase Cbotu_EstA from the anaerobe *Clostridium botulinum* ATCC 3502 (PDB: 5AH1) was found to hydrolyze the polyester poly(butylene adipate-co-butylene terephthalate)(PBAT)[28]. Because S9_948 was expressed and secreted in *BL21(DE3)* with low level, we used crude S9_948 in the following enzyme activity analysis.

To evaluate the PET-degrading activity of S9_948 and PHB, we carried out degradation assays using *p*-NPB, FDBz, and PET films as the substrates. As we expected, S9_948 and PHB exhibited significant kinetic hydrolytic activity against FDBz, compared to the blank control (**Fig. 5A**). Crude S9_948 and PHB also showed strong hydrolytic activities of 134.34±32.91 U·mL-1 and 91.96±24.19 U·mL-1 against *p*-NPB, respectively (**Fig. 5B**). Moreover, the SEM images reveal that both S9-948 and PHB can induce surface erosion to PET films after incubated for two weeks (**Fig. 5C**). However, the HPLC results of the relevant supernatants showed that hydrolysis products, including BHET, MHET, and TPA, are nondetectable. This result suggests that the enzymes might have low thermostability during long-term incubation or the activities of the enzymes are low. The above degradation assays suggest that S9_948 and PHB are potentially participating enzymes involved in the biodegradation of PET by Un-5 and Un-C2-8. Considering the complexity of the PET biodegradation process, we expect that other key PETases are yet to be discovered for the microbial isolates obtained by FADS.

4. Conclusion

In summary, to advance the discovery of PET-degrading enzymes for biodegradation and sustainable recycling of PET, we developed a complete FADS pipeline using FDBz as the fluorogenic probe for screening of single microbial cells at a large scale. We developed and optimized the pipeline to include long-term pre-incubation following microfluidic picoinjection

of the fluorescence substrate FDBz. Environmental microbes take more prolonged incubation compared with benchmark engineered strains. We then applied the system to screen an environmental sample from a PET textile mill, successfully obtained PET-degrading microbes belonging to 9 different genera. Moreover, two putative PETases from environmental microbial strains *K. endophyticus* Un-5 and *S. epidermidis* Un-C2-8 were genetically derived, heterologously expressed, and preliminarily validated for their PET-degrading activity. Overall, the FADS pipeline opens possibilities for obtaining novel microorganisms and enzymes for PET biodegradation with superior throughput, sensitivity, and specificity. The pipeline allows the directed evolution of PETases by random mutagenesis and screening. Moreover, it also enables direct screening of environmental microbes to recover novel enzymes that are not previously known or studied.

Our results prove that the FADS method could be applied and effectively speed up the screening of environmental microbes that exist in various environments. The presented methodology may be extended for screening degrading enzymes of other synthetic plastics such as polyesters[29-30], polyethylene[31-32], and polycarbonate[33], with further development of specific fluorogenic probes targeting various synthetic plastics. Besides, nano/micro-scale polymer particles coupling with fluorogenic enzymatic activity sensors are preferred to mimic the crystalline structures of plastic polymers in future work. To implement the FADS system in standard microbiology laboratories, we should focus on streamlining the instrument setup, device fabrication, and process automation.

5. Experimental

5.1 Materials

Terephthalic acid (TPA, Aladdin), 4-(*p*-nitrophenyl butyrate (*p*-NPB, Sigma), dimethyl sulfoxide (DMSO, Sigma) were acquired commercially. PET fibers, PET films, BHET, and MHET, were provided by Novozymes A/S (Denmark). Fluorescein dibenzoate (FDBz) was synthesized by Novozymes (see supporting information for details)[34]. A 10 mM stock solution of

FDBz in DMSO is prepared and diluted to the working concentration using 10 mM Tris-HCl (pH 7.4) for all experiments unless otherwise indicated. 'StickAway' cutinase and 'Lipex' lipase, both from Novozymes, were individually diluted in 10 mM Tris-HCl (pH 7.4) at a final concentration of 5 μM, and used to evaluate the performance of FDBz as a PET-degrading indicator. Quantitative measurements of FDBz and *p*-NPB hydrolysis by enzymes or microbial strains were performed using a fluorescence reader (EnSpire multimode plate Reader, Perkin Elmer, Waltham, USA). Countess™ cell counting chamber slides (Thermo Fisher Scientific, MA, USA) were used for droplet array imaging under the microscope. Low melting-temperature liquid solder (Indium, Clinton, NY, USA) was used for making electrodes on microfluidic devices

5.2 Microbial samples and preparation of cell suspensions

Wastewater samples were collected from a PET textile mill located in Southeast China (Shaoxing, Zhejiang, China) and stored at 4 °C until use. We diluted each 10 g sample in with 90 mL 1X PBS (pH 7.0) in a 250 mL flask and shaken at room temperature by 200 RPM for 30 min. Then 1 mL diluted sample solution was added into PET-YSV medium (PET fiber 6 g/L, $(NH_4)_2SO_4$ 0.2%, Trace elements 10%) for either direct FADS or FADS after enrichment cultivation. For enrichment cultivation, trace elements contain 0.1% $FeSO_4{\cdot}7H_2O$, 0.1% $MgSO_4{\cdot}7H_2O$, 0.01% $CuSO_4{\cdot}H_2O$, 0.01% $MnSO_4{\cdot}H_2O$ and 0.01% $ZnSO_4{\cdot}7H_2O$. The samples were cultivated for seven days at 37 °C before FADS. Live-cell numbers of the original sample or its enrichment were adjusted to similar levels via live/dead staining and cell counting (Live/Dead BacLight Bacterial Viability kit, Molecular Probes), and diluted to ~7×10^7 CFU·mL^{-1} in YSV medium to yield an average number of cells per droplet (λ) of 0.28 for single-cell sorting experiments.

5.3 Microfluidic device fabrication and operations

The optical setup for the FADS experiment is built based on an inverted microscope (IX81, Olympus, Japan)[20]. A 20 mW, 473 nm solid-state laser was shaped through a 20X objective into a

20 μm size spot, focusing in the sorting channel. Fluorescence of droplets was captured by the objective and split between a high-speed camera and a photomultiplier tube (10722-210, Hamamatsu Photonics). The signal output from the PMT was received and processed using a program written in LabVIEW (National Instrument, Austin, Texas, USA). Droplet sorting was triggered by a train of 1000-V, 30kHz pulses applied by a high voltage amplifier (Trek). Polydimethylsiloxane (PDMS) was purchased from Momentive Performance Materials (Waterford, NY). Microfluidic devices were designed and fabricated as previously described procedure. Gastight glass syringes (Agilent, Reno, NV) were used for loading and infusing solutions into the devices by Syringe Pumps (Harvard Apparatus, USA). Three devices, including the droplet maker, the picoinjector, and the droplet sorter, were operated step-by-step as follows: **(*i*)** droplet maker: microbial suspension samples were diluted to ~7×10^7 CFU/mL in YSV medium and infused into droplet maker device to generate single-cell encapsulating droplets (~4 pL) at a throughput of 2700 drops per second. The droplets were collected in a 20-cm long tubing and incubated for three days to produce PET-degrading enzymes by positive microbial species. **(*ii*)** picoinjection: Solution of FDBz was introduced into the droplets by picoinjection and incubated for 2 hours. **(*iii*)** droplet sorter: the droplets were sorted based on the fluorescent intensity at a throughput of ~420 drops per second for several hours (>2,560,000 droplets per hour), and those droplets with fluorescence above the sorting threshold were collected in an Eppendorf tube, following with demulsification and recovery of microbial cells for cultivation and enzymatic assays on agar plates. The fluorescence images of droplets were collected by an inverted fluorescence microscope (Eclipse Ti, Nikon, Tokyo, Japan).

5.4 High-throughput sequencing and phylogenetic analysis

Bacterial single colonies were picked from agar plates and inoculated in PET-YSV medium for subculture. DNA extractions from the isolates were carried out by using BMamp Rapid Bacterial DNA extraction kit (Cat. No. DL111-01, Biomed, Beijing, China) following the manufacturer's instructions. Following PCR-amplified 16S rRNA gene sequencing, EzBioCloud

(https://www.ezbiocloud.net/) was used to obtain 16S rRNA identity of the obtained strains. We use ClustalW to align the sequences, and we plotted the phylogenetic tree by MEGA6 software using the neighbor-joining method[35]. For whole-genome sequencing of pure isolates, DNA extractions were sequenced on an IlluminaHiSeq PE150 platform (Novogene Co., Beijing, China).

5.5 Validation of PET-degradation activity by clear zone formation and HPLC

The obtained microbial isolates were cultured in YSV medium added with PET fibers for three days, following by clear zone formation in a solid media plate assay. The BHET-Basal agar plates were prepared with 0.4% BHET and 25mM Tris-HCl (pH 7.4) in 1.5% agar. And the BHET-LB agar plates were prepared with 0.4% BHET and LB broth in 1.5% agar. Aliquots of 100 μL bacterial suspension from the YSV culture were added in punched holes on these agar plates and incubated at 37 °C, and the sizes of clear zones around the punched holes were measured after three days. Reverse-phase high-performance liquid chromatography (HPLC) was performed on an Agilent 1200 system (Agilent, Reno, NV) with a UV detector and a C18 column (Inertsil ODS-3, Shimadzu, Japan) as previously described[3]. The operation was carried out using a gradient (methanol-20 mM phosphate buffer) that increased from 25-100% at 15-25 min with a flow of 1 $mL \cdot min^{-1}$. The injection volume was 10 μL, and the detection wavelength was 240 nm.

5.6 Physicochemical and morphological characterization

A simultaneous thermal analyzer (NETZSCH STA 449F3, Germany) was used to perform thermogravimetric analysis (TGA) and differential thermal analysis (DTA) of PET fibers and films by heating 10~30 mg samples in an aluminum pan from 50 to 550 °C at 20 $K \cdot min^{-1}$. The crystal structures of PET samples were quantified using an X-ray powder diffractometer (XRD) (SmartLab, Rigaku, Japan). For SEM imaging, the PET films were cleaned, air-dried, and coated by gold sputtering and observed under a SU8010 scanning electron microscope (SEM, Hitachi, Japan) at 5 kV to unveil surface degradation structures.

5.7 Heterologous expression and preliminary validation of PET-degrading enzymes

The genes encoding putative PET-degrading enzymes, including S9_948 and PHB from *Kineococcus endophyticus* Un-5 and *Staphylococcus epidermidis* Un-C2-8 were selected for molecular cloning and heterologous expression. A set of specific primers were designed for PCR amplification of the target genes (Table S2). The PCR products were purified by agarose gel electrophoresis and sequenced for confirmation. Afterward, the target gene was connected to the expression vector pET-28a (Novagen) and transformed to *Escherichia coli* (*E. Coli*) *BL21(DE3)*. The recombinant putative enzymes were expressed as N-terminal fusion to His-tag. The transformed *BL21(DE3)* was cultured at 37 °C in 50 mL LB supplemented with 50 $\mu g \cdot mL^{-1}$ Kanamycin to reached an OD_{600} of 0.6, and then enzyme expression was induced at 16 °C overnight with shaking at 160 RPM. Following the induction time, cells were harvested by centrifugation and resuspended in 5 mL standard buffer (50 mM Tris-HCl (pH 8.0), 50 mM NaCl). Resuspended cells were lysed by an ultrasonic homogenizer (scientz-IID, Scientz Biotech, Ningbo, China) for 20 min. The supernatant (soluble fraction) containing the crude enzymes was separated from cell debris by centrifugation at 14,000 × g for 10 min and stored at 4 °C for further use.

The FDBz hydrolysis by crude S9_948 or PHB was performed by mixing 100-μL enzyme solution with 100-μL 250 μM FDBz. The kinetic assay was carried out using the EnSpire plate reader at 37 °C within 60 min. The hydrolysis of *p*-NPB by crude S9_948 or PHB were measured as previously described with slight modifications[36]. Absorbance assays were carried out on the EnSpire plate reader, using 200 μL reactions composed of 20 μL crude enzymes and 10 μL 1 M *p*-NPB in Tris buffer (pH 8.0). The production of *p*-nitrophenol (*p*-NP) was monitored at 405 nm within 20 min at 37 ^{o}C. One unit of activity (1 U) was defined as the enzymatic production of 1 μmol *p*-NP per min at 37 °C. The degradation of PET film by the crude S9_948 or PHB was evaluated by incubating PET film with the enzyme for seven days at 37 °C, and evaluated by morphological characterization as described above.

References:

1. Ammendolia, J.; Saturno, J.; Brooks, A. L.; Jacobs, S.; Jambeck, J. R., An emerging source of plastic pollution: Environmental presence of plastic personal protective equipment (PPE) debris related to COVID-19 in a metropolitan city. *Environ. Pollut.* **2021**, 269, 116160.
2. Geyer, R.; Jambeck, J. R.; Law, K. L., Production, use, and fate of all plastics ever made. *Sci. Adv.* **2017**, 3, e1700782.
3. Yoshida, S.; Hiraga, K.; Takehana, T.; Taniguchi, I.; Yamaji, H.; Maeda, Y.; Toyohara, K.; Miyamoto, K.; Kimura, Y.; Oda, K., A bacterium that degrades and assimilates poly(ethylene terephthalate). *Science* **2016**, 351, 1196-1199.
4. Ribitsch, D.; Acero, E. H.; Greimel, K.; Eiteljoerg, I.; Trotscha, E.; Freddi, G.; Schwab, H.; Guebitz, G. M., Characterization of a new cutinase from Thermobifida alba for PET-surface hydrolysis. *Biocatalysis* **2012**, 30, 2-9.
5. Hu, X.; Thumarat, U.; Zhang, X.; Tang, M.; Kawai, F., Diversity of polyester-degrading bacteria in compost and molecular analysis of a thermoactive esterase from Thermobifida alba AHK119. *Appl. Microbiol. Biot.* **2010**, 87, 771-779.
6. Carniel, A.; Valoni, R.; Junior, J. N.; Gomes, A. D. C.; Castro, A., Lipase from Candida antarctica (CALB) and cutinase from Humicola insolens act synergistically for PET hydrolysis to terephthalic acid. *Process Biochem.* **2017**, 59, 84-90.
7. Costa, A.; Lopes, V.; Vidal, L.; Nicaud, J. M.; Coelho, M., Poly(ethylene terephthalate) (PET) degradation by Yarrowia lipolytica: Investigations on cell growth, enzyme production and monomers consumption. *Process Biochem.* **2020**, 95, 81-90.
8. Koshti, R.; Mehta, L.; Samarth, N., Biological Recycling of Polyethylene Terephthalate: A Mini-Review. *J. Polym. Environ.* **2018**, 26, 3520-3529.
9. Cui, Y.; Chen, Y.; Liu, X.; Dong, S.; Wu, B., Computational Redesign of a PETase for Plastic Biodegradation under Ambient Condition by the GRAPE Strategy. *ACS Catal.* **2021**, 11, 1340-1350.

10. Sagong, H. Y.; Seo, H.; Kim, T.; Son, H. F.; Kim, K. J., Decomposition of PET film by MHETase using Exo-PETase function. *ACS Catal.* **2020**, 10, 4805-4812.
11. Tournier, V.; Topham, C. M.; Gilles, A.; David, B.; Folgoas, C.; Moya-Leclair, E.; Kamionka, E.; Desrousseaux, M. L.; Texier, H.; Gavalda, S.; Cot, M.; Guemard, E.; Dalibey, M.; Nomme, J.; Cioci, G.; Barbe, S.; Chateau, M.; Andre, I.; Duquesne, S.; Marty, A., An engineered PET depolymerase to break down and recycle plastic bottles. *Nature* **2020**, 580, 216-219.
12. Shinozaki, Y.; Watanabe, T.; Nakajima-Kambe, T.; Kitamoto, H. K., Rapid and simple colorimetric assay for detecting the enzymatic degradation of biodegradable plastic films. *J. Biosci. Bioeng.* **2013**, 115, 111-114.
13. Thumarat, U.; Nakamura, R.; Kawabata, T.; Suzuki, H.; Kawai, F., Biochemical and genetic analysis of a cutinase-type polyesterase from a thermophilic Thermobifida alba AHK119. *Appl. Microbiol. Biot.* **2012**, 95, 419-430.
14. Wei, R.; Oeser, T.; Schmidt, J.; Meier, R.; Barth, M.; Then, J.; Zimmermann, W., Engineered bacterial polyester hydrolases efficiently degrade polyethylene terephthalate due to relieved product inhibition. *Biotechnol. Bioeng.* **2016**, 113, 1658-1665.
15. Zhong-Johnson, E.; Voigt, C. A.; Sinskey, A. J., An absorbance method for analysis of enzymatic degradation kinetics of poly(ethylene terephthalate) films. *Sci. Rep.* **2021**, 11, 928.
16. Markel, U.; Essani, K. D.; Besirlioglu, V.; Schiffels, J.; Streit, W. R.; Schwaneberg, U., Advances in ultrahigh-throughput screening for directed enzyme evolution. *Chem. Soc. Rev.* **2020**, 49, 233-262.
17. de Rond, T.; Danielewicz, M.; Northen, T., High throughput screening of enzyme activity with mass spectrometry imaging. *Curr. Opin. Biotech.* **2015**, 31, 1-9.
18. Obexer, R.; Pott, M.; Zeymer, C.; Griffiths, A. D.; Hilvert, D., Efficient laboratory evolution of computationally designed enzymes with low starting activities using fluorescence-activated droplet sorting. *Protein Eng. Des. Sel.* **2016**, 29, 355-366.
19. Baret, J. C.; Miller, O. J.; Taly, V.; Ryckelynck, M.; El-Harrak, A.; Frenz, L.; Rick, C.; Samuels, M. L.; Hutchison, J. B.; Agresti, J. J.; Link, D. R.; Weitz, D. A.; Griffiths, A. D.,

Fluorescence-activated droplet sorting (FADS): efficient microfluidic cell sorting based on enzymatic activity. *Lab Chip* **2009**, 9, 1850-1858.

20. Qiao, Y.; Zhao, X.; Zhu, J.; Tu, R.; Dong, L.; Wang, L.; Dong, Z.; Wang, Q.; Du W, Fluorescence-activated droplet sorting of lipolytic microorganisms using a compact optical system. *Lab Chip* **2017**, 18, 190-196.
21. Vallejo, D.; Nikoomanzar, A.; Paegel, B. M.; Chaput, J. C., Fluorescence-Activated Droplet Sorting for Single-Cell Directed Evolution. *ACS Synth. Biol.* **2019**, 8, 1430-1440.
22. Najah, M.; Calbrix, R.; Mahendra-Wijaya, I. P.; Beneyton, T.; Griffiths, A. D.; Drevelle, A., Droplet-based microfluidics platform for ultra-high-throughput bioprospecting of cellulolytic microorganisms. *Chem. Biol.* **2014**, 21, 1722-1732.
23. Goto, H.; Kanai, Y.; Yotsui, A.; Shimokihara, S.; Shitara, S.; Oyobiki, R.; Fujiwara, K.; Watanabe, T.; Einaga, Y.; Matsumoto, Y.; Miki, N.; Doi, N., Microfluidic screening system based on boron-doped diamond electrodes and dielectrophoretic sorting for directed evolution of NAD(P)-dependent oxidoreductases. *Lab Chip* **2020**, 20, 852-861.
24. Sjostrom, S. L.; Bai, Y.; Huang, M.; Liu, Z.; Nielsen, J.; Joensson, H. N.; Andersson, S. H., High-throughput screening for industrial enzyme production hosts by droplet microfluidics. *Lab Chip* **2014**, 14, 806-813.
25. He, F. Y.; Wang, L. F.; Li, B. R.; Wang, Q. G.; Wang, Q., Studies on crystal structure and hydrolysis feature of the fluorescein dibenzoate. *Acta Chim. Sinica* **1993**, 51, 119-124.
26. Ma, J.; Wu, L.; Guo, F.; Gu, J.; Tang, X.; Jiang, L.; Liu, J.; Zhou, J.; Yu, H., Enhanced enantioselectivity of a carboxyl esterase from Rhodobacter sphaeroides by directed evolution. *Appl Microbiol Biotechnol* **2013**, 97, 4897-4906.
27. Okano, H.; Hong, X.; Kanaya, E.; Angkawidjaja, C.; Kanaya, S., Structural and biochemical characterization of a metagenome-derived esterase with a long N-terminal extension. *Protein Sci.* **2015**, 24, 93-104.
28. Perz, V.; Baumschlager, A.; Bleymaier, K.; Zitzenbacher, S.; Hromic, A.; Steinkellner, G.; Pairitsch, A.; Lyskowski, A.; Gruber, K.; Sinkel, C.; Kuper, U.; Ribitsch, D.; Guebitz, G. M.,

Hydrolysis of synthetic polyesters by Clostridium botulinum esterases. *Biotechnol. Bioeng.* **2016**, 113, 1024-1034.

29. DelRe, C.; Jiang, Y.; Kang, P.; Kwon, J.; Hall, A.; Jayapurna, I.; Ruan, Z.; Ma, L.; Zolkin, K.; Li, T.; Scown, C. D.; Ritchie, R. O.; Russell, T. P.; Xu, T., Near-complete depolymerization of polyesters with nano-dispersed enzymes. *Nature* **2021**, 592, 558-563.
30. Zadjelovic, V.; Chhun, A.; Quareshy, M.; Silvano, E.; Hernandez Fernaud, J. R.; Aguilo Ferretjans, M. M.; Bosch, R.; Dorador, C.; Gibson, M. I.; Christie Oleza, J. A., Beyond oil degradation: enzymatic potential ofAlcanivorax to degrade natural and synthetic polyesters. *Environ. Microbiol.* **2020**, 22, 1356-1369.
31. Yang, J.; Yang, Y.; Wu, W. M.; Zhao, J.; Jiang, L., Evidence of polyethylene biodegradation by bacterial strains from the guts of plastic-eating waxworms. *Environ. Sci. Technol.* **2014**, 48, 13776-13784.
32. Tennakoon, A.; Wu, X.; Paterson, A. L.; Patnaik, S.; Pei, Y.; LaPointe, A. M.; Ammal, S. C.; Hackler, R. A.; Heyden, A.; Slowing, I. I.; Coates, G. W.; Delferro, M.; Peters, B.; Huang, W.; Sadow, A. D.; Perras, F. A.; Ames Lab., A. I. U. S.; Argonne National Lab. ANL, A. I. U. S., Catalytic upcycling of high-density polyethylene via a processive mechanism. *Nat. Catal.* **2020**, 3, 893-901.
33. Artham, T.; Doble, M., Biodegradation of physicochemically treated polycarbonate by fungi. *Biomacromolecules* **2010**, 11, 20-28.
34. Poznik, M.; Konig, B., Cooperative hydrolysis of aryl esters on functionalized membrane surfaces and in micellar solutions. *Org. Biomol. Chem.* **2014**, 12, 3175-3180.
35. Tamura, K.; Stecher, G.; Peterson, D.; Filipski, A.; Kumar, S., MEGA6: Molecular Evolutionary Genetics Analysis version 6.0. *Mol. Biol. Evol.* **2013**, 30, 2725-2729.
36. Ate Lier, Z.; Metin, K., Production and Partial Characterization of a Novel Thermostable Esterase from a Thermophilic Bacillus sp. *Enzyme Microb. Tech.* **2006**, 38, 628-635.

Acknowledgment

We thank Prof. Bian Wu from the Institute of Microbiology Chiese Academy of Sciences for his helpful discussion. This study was supported by the National Natural Science Foundation of China (21822408, 91951103, 31970091, 52073004), the Key Program of Frontier Sciences of the Chinese Academy of Sciences (QYZDB-SSW SMC008), the National Key Research and Development Program of China (2018YFC0310703), the Senior User Project of RV KEXUE from the Center for Ocean Mega-Science, Chinese Academy of Sciences (KEXUE2019GZ05), and the Open Foundation of Beijing Key Laboratory of Quality Evaluation Technology for Hygiene and Safety of Plastics (PQETGP2020003).

Conflicts of interest: Authors declare no competing interests.

Supplementary Materials:

Materials and Methods

Tables S1-S2

Figures S1-S9

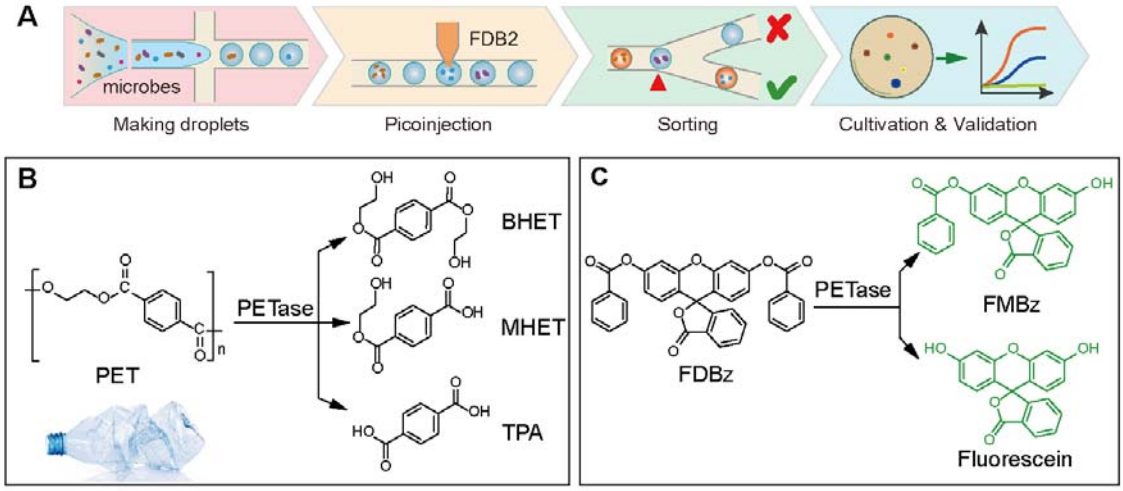

Figure 1. The workflow for sorting PET-degrading microbes by droplet microfluidics using Fluorescein dibenzoate (FDBz) as the fluorogenic substrate. (A) The sorting procedures. (B) The biodegradation of PET by PETases releases MHET, BHET, and TPA. (C) Hydrolysis of FDBz releases FMBz and fluorescein.

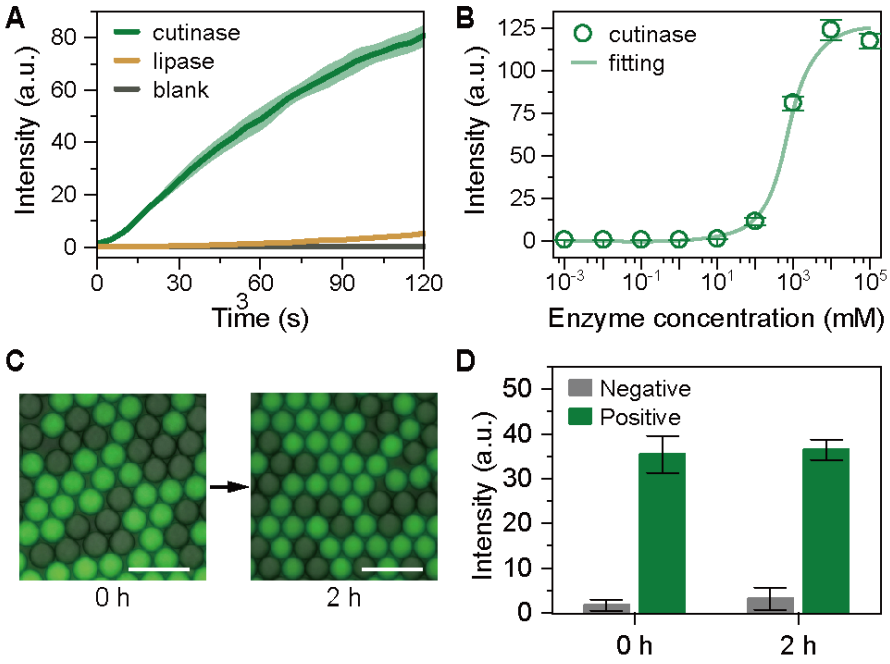

Figure 2. The FDBz-based fluorogenic assays for PETases. (A)The fluorescence reaction in the microplate. (B) Specificity and selectivity of cutinase-FDBz hydrolysis compare with lipase and blank control. (C) FDBz-based fluorogenic assays in 4 pL droplets were indicating high sensitivity, low leakage, and low self-hydrolysis. (D) fluorescence intensity difference between cutinase-FDBz and lipase-FDBz droplets before and after 2-h incubation. (Scale bar: 50 μm)

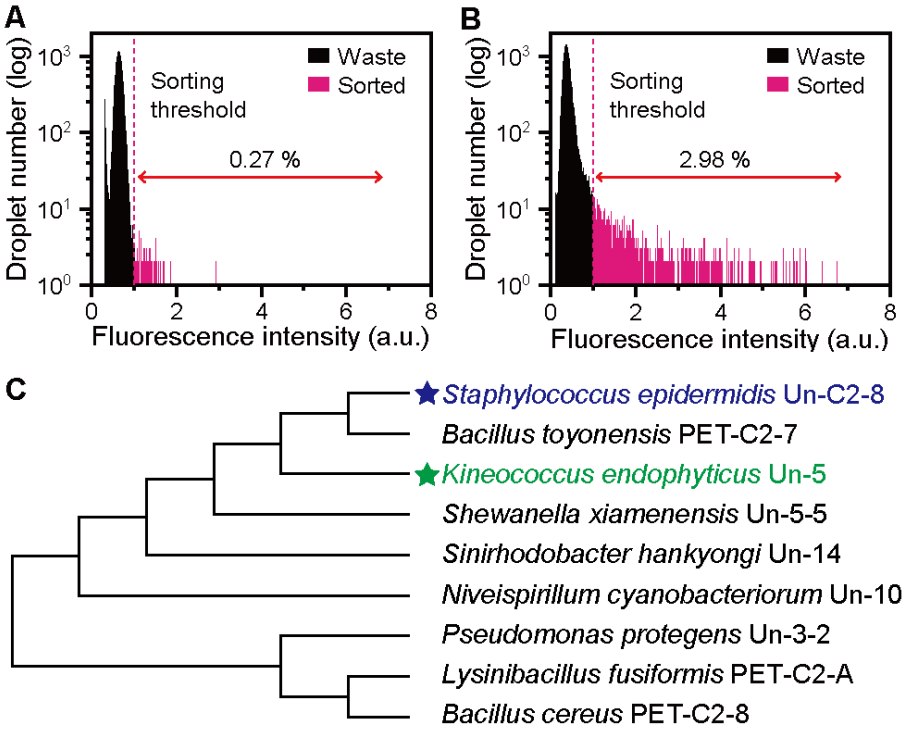

Figure 3. FADS of PET degraders from wastewater of a PET textile mill. Histograms showing droplet fluorescence of the original (A) and PET-YSV enriched (B) cell suspensions. The pink dashed lines indicate the sorting threshold. (C) The phylogenetic tree of PET-degrading strains obtained by FADS from PET textile mill wastewater.

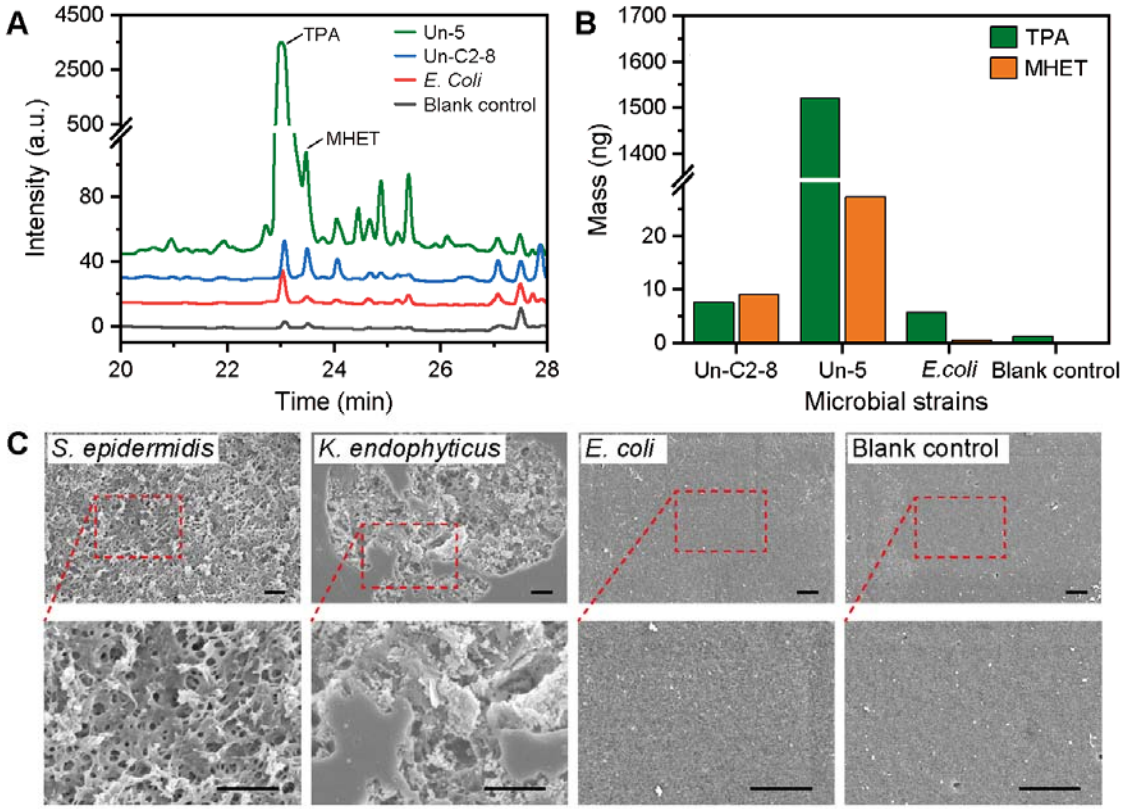

Figure 4. Validation of PET-biodegradation by FADS-obtained isolates *K. endophyticus* Un-5 and *S. epidermidis* Un-C2-8. (A) HPLC spectra of the degrading products released from the PET film incubated with Un-5, Un-C2-8, *E. coli*, and the blank control. (B) Mass conversion of PET film to TPA and MHET detected in culture supernatants from different strains and the blank control. (C) SEM images of PET films after 2-week degradation experiments with different strains compared with the blank.

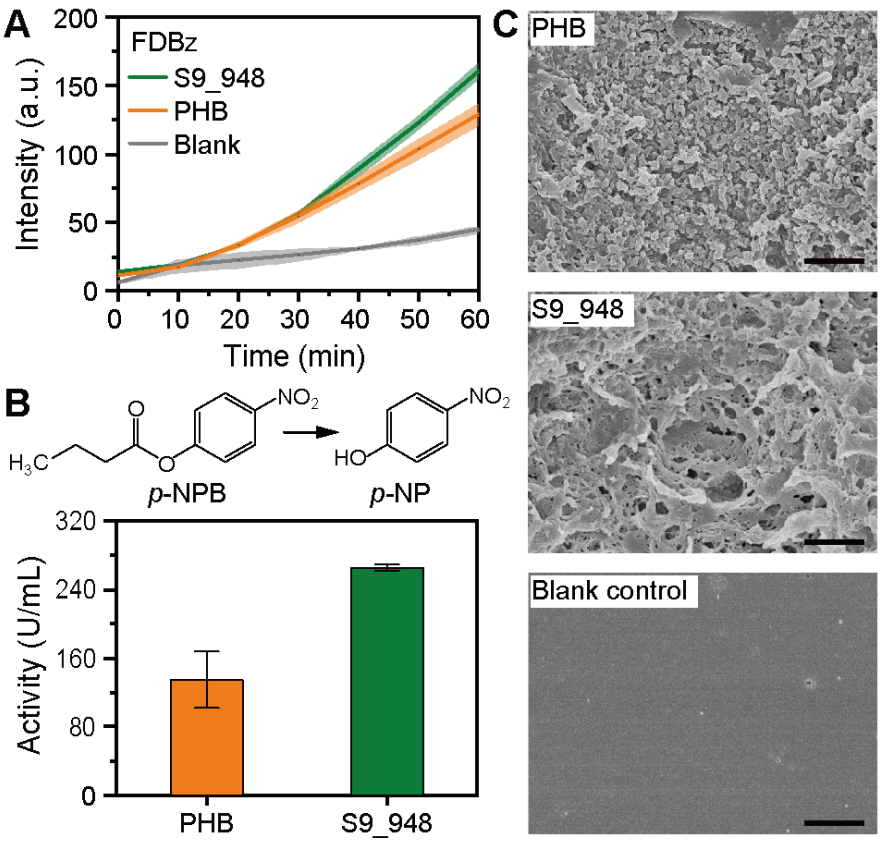

Figure 5. Enzymatic activity of PHB and S9_948. (A) hydrolysis of *p*-NPB measured by absorbance; (B) hydrolysis of FDBz measured by fluorescence plate reader; (C) SEM images show surface erosion of PET films.